Rescuing leptogenesis in inverse seesaw models with the help of non-Abelian flavor symmetries

Yan Shao and Zhen-hua Zhao*

Department of Physics, Liaoning Normal University, Dalian 116029, China and Center for Theoretical and Experimental High Energy Physics, Liaoning Normal University, Dalian 116029, China

(Received 3 November 2025; accepted 18 December 2025; published 2 January 2026)

The inverse seesaw (ISS) model provides an attractive framework that can naturally explain the smallness of neutrino masses while accommodating some sterile neutrinos potentially accessible at present or future experiments. However, in generic ISS models with hierarchical pseudo-Dirac (PD) sterile neutrino pairs, the generation of the observed baryon asymmetry of the Universe via the leptogenesis mechanism is extremely challenging. In this paper, we investigate rescuing leptogenesis in the ISS model with the help of non-Abelian flavor symmetries, which have the potential to explain the observed peculiar neutrino mixing pattern: we first implement non-Abelian flavor symmetries to naturally enforce mass degeneracies among different pseudo-Dirac sterile neutrino pairs and then break them in a proper way so that resonant leptogenesis among different PD sterile neutrino pairs can arise, thus enhancing the generated baryon asymmetry. To be specific, we have considered the following two well-motivated approaches for generating the tiny mass splittings among different PD sterile neutrino pairs: one approach makes use of the renormalization-group corrections to the sterile neutrino masses, while the other approach invokes nontrivial flavor structure of the μ_s matrix. For these two scenarios, we aim to explore the viability of leptogenesis and to identify the conditions under which the observed baryon asymmetry can be successfully reproduced.

DOI: 10.1103/8pl4-nrkf

I. INTRODUCTION

The Standard Model (SM) of particle physics, while being incredibly successful, fails to address two fundamental puzzles: the origin of neutrino masses and the generation of the baryon-antibaryon asymmetry of the Universe (BAU). On the one hand, neutrino oscillations have conclusively demonstrated that neutrinos have nonzero masses [1], which contradicts the Standard Model's assumption of massless neutrinos. On the other hand, the BAU puzzle, quantified as [2]

$$Y_{\mathrm{B}} \equiv \frac{n_{\mathrm{B}} - n_{\overline{\mathrm{B}}}}{s} \simeq (8.69 \pm 0.04) \times 10^{-11}, \qquad (1)$$

where n_{B} ($n_{\overline{\mathrm{B}}}$) denotes the baryon (antibaryon) number density and s the entropy density, remains unresolved.

One of the most popular and natural ways to generate the tiny neutrino masses is via the type-I seesaw mechanism [3–7], which introduces at least two heavy right-handed neutrinos (RHNs) N_I (for $I = 1, 2, \ldots$) into the SM. With the help of this mechanism, the smallness of neutrino masses can be naturally ascribed to the heaviness of RHNs. Furthermore, the type-I seesaw model also provides an elegant solution to the BAU puzzle via the leptogenesis mechanism [8–12]: a lepton asymmetry is first generated from the *CP*-violating and out-of-equilibrium decays of RHNs and then partially converted to the desired baryon asymmetry via the sphaleron processes. However, the traditional type-I seesaw mechanism and associated leptogenesis mechanism have the drawback that the newly introduced particle states (i.e., RHNs) are too heavy to be directly accessed by foreseeable experiments: on the one hand, in order to naturally generate eV-scale neutrino masses, the RHN masses need to be around $\mathcal{O}(10^{13})$ GeV; on the other hand, when the RHN masses are hierarchial, in order to generate sufficient baryon asymmetry, the lightest RHN mass needs to be above $\mathcal{O}(10^{9})$ GeV [13].

In order to make the seesaw scale potentially accessible at present or future experiments, the inverse seesaw (ISS) model offers an elegant alternative [14,15]. In addition to the RHNs, the model also introduces some other singlet fermions S_I (for $I = 1, 2, \ldots$), and there are the following Lagrangian terms relevant for the generation of neutrino masses:

*Contact author: zhaozhenhua@lnnu.edu.cn

Published by the American Physical Society under the terms of the Creative Commons Attribution 4.0 International license. Further distribution of this work must maintain attribution to the author(s) and the published article's title, journal citation, and DOI. Funded by SCOAP³.

$$-\mathcal{L}_{\rm mass} \supset (Y_\nu)_{\alpha I}\overline{L_\alpha}\,\tilde{H}\,N_I + (M_{\rm R})_{IJ}\overline{N_I^c}S_J^c + \frac{1}{2}(\mu_{\rm s})_{IJ}\overline{S_I}S_J^c + {\rm H.c.}, \tag{2}$$

where L_α (for $\alpha = e, \mu, \tau$) and H (for $\tilde{H} = {\rm i}\sigma_2 H^*$ with σ_2 being the second Pauli matrix), respectively, denote the lepton and Higgs doublets, and the superscript c denotes the charge conjugated fields, and Y_ν, $M_{\rm R}$ and $\mu_{\rm s}$ are Yukawa and mass matrices in the flavor space. After the Higgs field acquires its vacuum expectation value $v = 174$ GeV, the Yukawa couplings will lead to some mass terms connecting the left-handed neutrinos ν_α and RHNs: $(M_{\rm D})_{\alpha I} = (Y_\nu)_{\alpha I} v$. In the $(\nu_\alpha^c, N_I, S_I^c)$ basis, the complete neutrino mass matrix is thus given by

$$M_{\nu NS} = \begin{pmatrix} 0 & M_{\rm D} & 0 \\ M_{\rm D}^T & 0 & M_{\rm R} \\ 0 & M_{\rm R}^T & \mu_{\rm s} \end{pmatrix}. \tag{3}$$

In this model the lepton number is violated by the Majorana mass terms of S_I, so the $\mu_{\rm s}$ parameters can be naturally small in the sense of 't Hooft [16] (i.e., the lepton number symmetry would get restored in the limit of $\mu_{\rm s} \to 0$). Under the natural condition of $\mu_{\rm s} \ll M_{\rm D} \ll M_{\rm R}$, the light neutrino masses can be derived by performing a block diagonalization of Eq. (3):

$$M_\nu = M_{\rm D}(M_{\rm R}^T)^{-1}\mu_{\rm s}M_{\rm R}^{-1}M_{\rm D}^T. \tag{4}$$

We see that the smallness of neutrino masses follows naturally from small values of $\mu_{\rm s}$, rendering superheavy RHNs no longer necessary. This can be intuitively understood from the following numerical relation:

$$\left(\frac{M_\nu}{0.1\ {\rm eV}}\right) = \left(\frac{M_{\rm D}}{100\ {\rm GeV}}\right)^2\left(\frac{\mu_{\rm s}}{1\ {\rm keV}}\right)\left(\frac{M_{\rm R}}{10\ {\rm TeV}}\right)^{-2}, \tag{5}$$

which shows that the RHN mass scale can be naturally lowered to the TeV range for reasonable values of $\mu_{\rm s}$ and $M_{\rm D}$. Therefore, the ISS model provides an attractive framework that can naturally explain the smallness of neutrino masses while accommodating some sterile neutrinos potentially accessible at present or future experiments (see, e.g., Refs. [17,18]).

On the other hand, the RHN and S_I singlets (collectively referred to as sterile neutrinos) can be reorganized into pseudo-Dirac (PD) sterile neutrino pairs [19–22]. While a Dirac sterile neutrino can be thought of as two exactly degenerate Majorana sterile neutrinos with opposite CP phases (which will be realized for $\mu_{\rm s} = 0$), a PD sterile neutrino pair contains two nearly degenerate Majorana mass eigenstates with a tiny mass splitting (which will be realized for small values of $\mu_{\rm s}$). To be concrete, in the one-generation sterile neutrino scenario (with only a pair of N_I and S_I), one will arrive at a pair of PD sterile neutrinos with the masses $M_{\rm R} + \mu_{\rm s}/2$ and $M_{\rm R} - \mu_{\rm s}/2$. When it is generalized to the multigeneration sterile neutrino scenario (with multiple pairs of N_I and S_I), one will similarly arrive at multiple pairs of PD sterile neutrinos, which have their respective central masses and mass splittings.

At first sight, it seems that the quasidegeneracy between a pair of PD sterile neutrinos is advantageous to the realization of resonant leptogenesis [23,24], which is expected to help us achieve a successful leptogenesis even with TeV scale sterile neutrinos. However, for generic ISS models with hierarchical PD sterile neutrino pairs (in which case the resonance effects for leptogenesis only take place within each pair of PD sterile neutrinos, in contrast with the scenario we will consider in this paper), the detailed study shows that the generated baryon asymmetry is smaller than its desired value by at least a few orders of magnitude [25]. This is mainly due to (i) partial cancellation of lepton asymmetries within each pair of PD sterile neutrinos and (ii) huge washout effects. In the literature, there already exist some studies on rescuing leptogenesis in the ISS model. For example, Refs. [26,27] have made use of the Akhmedov-Rubakov-Smirnov mechanism (i.e., oscillations of sterile neutrinos) [28,29] to do so, and Ref. [30] has considered a nonstandard cosmological expansion history and a quasidegenerate mass spectrum of sterile neutrinos to do so.

Reference [31] has pointed out that quasidegeneracies among different PD pairs could potentially enhance leptogenesis in the ISS framework, motivating us to examine whether such structures can arise naturally from an underlying flavor principle. In this paper, we investigate rescuing leptogenesis in the ISS model with the help of non-Abelian flavor symmetries which are motivated by the observed peculiar neutrino mixing pattern (see the next paragraph). Unlike previous studies such as Ref. [30], where the nearly degenerate PD sterile neutrinos are effectively introduced through an arbitrary choice of their mass parameters, in our setup the required mass degeneracies emerge naturally as a consequence of the non-Abelian flavor symmetry. These symmetries enforce a highly constrained texture for $M_{\rm R}$ [see Eq. (7)], thereby providing a theoretical origin for the exact degeneracy among the three PD pairs and simultaneously reducing the number of free parameters.

Historically, the facts that the neutrino mixing angles θ_{12} and θ_{23} are close to some special values (i.e., $\sin^2\theta_{12} \sim 1/3$ and $\sin^2\theta_{23} \sim 1/2$, see the global-fit results for the neutrino-oscillation experiments in Refs. [32,33]) and the smallness of θ_{13} suggest that the neutrino mixing matrix approximates to a very special form (which is referred to as the tribimaximal (TBM) mixing [34,35]) as

$$U_{\rm TBM} = \frac{1}{\sqrt{6}}\begin{pmatrix} -2 & \sqrt{2} & 0 \\ 0 & \sqrt{2} & -\sqrt{3} \\ 1 & \sqrt{2} & \sqrt{3} \end{pmatrix}, \tag{6}$$

which naturally predicts $\sin^2\theta_{12} = 1/3$, $\sin^2\theta_{23} = 1/2$, and $\theta_{13} = 0$. Such a remarkably simple and compact neutrino mixing pattern has attracted people to believe that there exists some flavor symmetry in the neutrino sector and have made a lot of attempts to explore the possible flavor symmetries (in particular, non-Abelian flavor symmetries such as the A_4 and S_4 groups) underlying the observed neutrino mixing pattern [36–40]. After the experimental determination of a relatively large θ_{13}, the TM1 (TM2) mixing [41–45], which retains the first (second) column of the TBM mixing while accommodating a nonzero θ_{13}, has become popular.

To be concrete, we propose a scenario in which mass degeneracies exist among different PD sterile neutrino pairs, which are then broken in a proper way. This configuration allows for resonant leptogenesis among different PD sterile neutrino pairs, potentially enhancing the generated baryon asymmetry. To achieve this, we utilize the above-mentioned non-Abelian flavor symmetries, which can naturally enforce mass degeneracies by unifying three RHNs (and also three S_I singlets) into a triplet representation (see, e.g., Refs. [46–51]). These symmetries ensure that the mass matrix $M_{\rm R}$ in Eq. (3) adopts a symmetric form as given by

$$M_{\rm R} = M_0 \begin{pmatrix} 1 & 0 & 0 \\ 0 & 0 & 1 \\ 0 & 1 & 0 \end{pmatrix}. \tag{7}$$

In order to achieve the desired particular neutrino mixing pattern such as TM1 (TM2), at least one of the mass matrices $M_{\rm D}$ and $\mu_{\rm s}$ must encode a nontrivial flavor structure. A minimal choice (see also Ref. [51]) is that the mass matrix $\mu_{\rm s}$ shares a same structure as $M_{\rm R}$ in Eq. (7):

$$\mu_{\rm s} = \mu_0 \begin{pmatrix} 1 & 0 & 0 \\ 0 & 0 & 1 \\ 0 & 1 & 0 \end{pmatrix}, \tag{8}$$

while $M_{\rm D}$ encodes a nontrivial flavor structure. For the sake of clarity, the structure of $M_{\rm D}$ is taken to have the following form:

$$M_{\rm D} = \begin{pmatrix} a & 2b & 2c \\ 2b & 4b+d & a-b-c-d \\ 2c & a-b-c-d & 4c+d \end{pmatrix}, \tag{9}$$

which will naturally realize the popular TM1 neutrino mixing. With the help of Eq. (4), utilizing the light neutrino mass matrix, which can be partially reconstructed in terms of the observed neutrino mixing angles and neutrino mass squared differences, we can derive the $M_{\rm D}$ matrix accordingly. This derivation allows us to proceed with the subsequent calculations of baryon asymmetry.

It is easy to see that, for $M_{\rm R}$ in Eq. (7) and $\mu_{\rm s}$ in Eq. (8), the masses of three PD sterile neutrino pairs are completely degenerate, with each pair split by μ_0:

$$\begin{aligned} M_1 = M_2 = M_3 &\simeq M_0 - \frac{1}{2}\mu_0, \\ M_4 = M_5 = M_6 &\simeq M_0 + \frac{1}{2}\mu_0. \end{aligned} \tag{10}$$

Then, as explained above, these degeneracies need to be broken in order for resonant leptogenesis among different PD sterile neutrino pairs to come into play. In this work, we consider the following two well-motivated approaches to generate such desired mass splittings: (i) they can be naturally induced by the renormalization group evolution (RGE) effects; (ii) when the mass matrix $\mu_{\rm s}$ also contains some nontrivial flavor structure parallel to that in Eq. (9) (so that the TM1 mixing scheme will be preserved), the flavor nonuniversality of $\mu_{\rm s}$ will break the mass degeneracies among the three PD sterile neutrino pairs. By analyzing these two scenarios, we aim to assess the viability of leptogenesis in the ISS model equipped with non-Abelian flavor symmetries and to identify the conditions under which the observed baryon asymmetry of the Universe can be successfully reproduced.

The remaining parts of this paper are organized as follows. In the next section, we recapitulate some basic formulas of ISS model and leptogenesis as a basis of our study. In Secs. III and IV, we separately investigate the potential for leptogenesis within the ISS model equipped with non-Abelian flavor symmetries under the two distinct scenarios outlined above. For these scenarios, we will also investigate the consequences of the model with respect to the charged lepton flavor violation processes. Finally, the summary of our main results will be given in Sec. V.

II. SOME BASIC FORMULAS OF ISS MODEL AND LEPTOGENSIS

In this section, we recapitulate some basic formulas of ISS model and leptogenesis as a basis of our study.

In order to facilitate the leptogenesis calculations, it is most convenient to work in the sterile neutrino mass basis, where the bottom-right submatrix of Eq. (3) (denoted as M_{NS}) becomes real, positive, and diagonal. For this purpose, one can diagonalize M_{NS} via the unitary transformation $V_{\rm R}$ [52],

$$V_{\rm R}^T M_{NS} V_{\rm R} \approx \begin{pmatrix} V_1^T\left[-M_{\rm R} + \frac{1}{2}\mu_{\rm s}\right]V_1 & 0 \\ 0 & V_2^T\left[M_{\rm R} + \frac{1}{2}\mu_{\rm s}\right]V_2 \end{pmatrix}, \tag{11}$$

with

$$V_{\mathrm{R}} \approx \frac{1}{\sqrt{2}} \begin{pmatrix} \mathbf{1}+\frac{\mu_{\mathrm{s}} M_{\mathrm{R}}^{-1}}{4} & \mathbf{1}-\frac{\mu_{\mathrm{s}} M_{\mathrm{R}}^{-1}}{4} \\ -\mathbf{1}+\frac{\mu_{\mathrm{s}} M_{\mathrm{R}}^{-1}}{4} & \mathbf{1}+\frac{\mu_{\mathrm{s}} M_{\mathrm{R}}^{-1}}{4} \end{pmatrix} \begin{pmatrix} V_1 & 0 \\ 0 & V_2 \end{pmatrix}, \tag{12}$$

where V_1 and V_2 are the unitary matrices for diagonalizing $-M_{\mathrm{R}}+1/2\mu_{\mathrm{s}}$ and $M_{\mathrm{R}}+1/2\mu_{\mathrm{s}}$, respectively. In this way the complete neutrino mass matrix is transformed to the following form:

$$M'_{\nu NS} \simeq \begin{pmatrix} 0 & vY'_{\mathrm{D}} & vY'_{\mathrm{L}} \\ v(Y'_{\mathrm{D}})^T & V_1^T\left[-M_{\mathrm{R}}+\frac{1}{2}\mu_{\mathrm{s}}\right]V_1 & 0 \\ v(Y'_{\mathrm{L}})^T & 0 & V_2^T\left[M_{\mathrm{R}}+\frac{1}{2}\mu_{\mathrm{s}}\right]V_2 \end{pmatrix}, \tag{13}$$

where Y'_{D} and Y'_{L} correspond to the rotated 3×3 Yukawa matrices that couple the sterile neutrinos to the SM leptons, and they can be analytically expressed as follows [53]:

$$Y'_{\mathrm{D}} \simeq \frac{1}{\sqrt{2}v}\left[M_{\mathrm{D}}\left(\mathbf{1}+\frac{\mu_{\mathrm{s}} M_{\mathrm{R}}^{-1}}{4}\right)V_1\right],$$
$$Y'_{\mathrm{L}} \simeq \frac{1}{\sqrt{2}v}\left[M_{\mathrm{D}}\left(\mathbf{1}-\frac{\mu_{\mathrm{s}} M_{\mathrm{R}}^{-1}}{4}\right)V_2\right]. \tag{14}$$

In the low-scale (TeV or so) leptogenesis regime, which we are interested in, all the three lepton flavors have become distinguishable from one another and the lepton asymmetries stored in them should be tracked separately [54,55]. On the other hand, the contributions of the nearly degenerate sterile neutrinos to the final baryon asymmetry are on the same footing and should be taken into consideration altogether. For these two reasons, the final baryon asymmetry can be obtained as

$$Y_{\mathrm{B}} = cY_{\mathrm{L}} = cr\sum_{\alpha}\varepsilon_\alpha\kappa_\alpha, \tag{15}$$

where $c \simeq -1/3$ is the conversion efficiency from the lepton asymmetry to the baryon asymmetry via the sphaleron processes, $r \simeq 4\times 10^{-3}$ measures the ratio of the equilibrium number density of sterile neutrinos to the entropy density, and ε_α is a sum over the sterile neutrinos (i.e., $\varepsilon_\alpha = \sum_I \varepsilon_{I\alpha}$) of the CP asymmetries for their decays:

$$\varepsilon_{I\alpha} \equiv \frac{\Gamma(N_I \to L_\alpha + H) - \Gamma(N_I \to \overline{L}_\alpha + \bar{H})}{\sum_\alpha \Gamma(N_I \to L_\alpha + H) + \Gamma(N_I \to \bar{L}_\alpha + \bar{H})}. \tag{16}$$

Finally, κ_α are the efficiency factors that take account of the washout effects due to the inverse decays of sterile neutrinos and various lepton-number-violating scattering processes. The explicit expressions for $\varepsilon_{I\alpha}$ and κ_α are given below.

In the resonant leptogenesis regime relevant for our study, which involves three pairs of PD sterile neutrinos (i.e., six nearly degenerate states), the CP asymmetries differ from the conventional two-state expressions. In particular, the effective neutrino Yukawa couplings in our framework are given by the following form [56–58]:

$$(\bar{h}_+)_{\alpha I} = h_{\alpha I} + \mathrm{i}\mathcal{V}_{\alpha I} - \mathrm{i}\sum_{J,K,L,M,N=1}^{6} h_{\alpha J}\mathcal{F}_{IJKLMN}, \tag{17}$$

where $h = (Y'_{\mathrm{D}}, Y'_{\mathrm{L}})$, and

$$\mathcal{V}_{\alpha I} = -\sum_{\beta=e,\mu,\tau}\sum_{J\neq I}\frac{h^*_{\beta I}h_{\beta J}h_{\alpha J}}{16\pi} f\left(\frac{M_J^2}{M_I^2}\right),$$
$$\mathcal{F}_{IJKLMN} = \frac{1}{(M_I^2 - M_J^2 + 2\mathrm{i}M_I^2 A_{JJ})F^{(4)}_{IJKLMN}} \times \Big\{ M_I(\mathcal{M}_{IIJ} + \mathcal{M}_{JJI})$$
$$- \mathrm{i}R_{IN}[\mathcal{M}_{INJ}(\mathcal{M}_{IIN} + \mathcal{M}_{NNI}) + \mathcal{M}_{JJN}(\mathcal{M}_{INI} + \mathcal{M}_{NIN})]$$
$$- \mathrm{i}R_{IM}\frac{1}{F^{(1)}_{IMN}}[\mathcal{M}_{IMJ}(\mathcal{M}_{IIM} + \mathcal{M}_{MMI}) + \mathcal{M}_{JJM}(\mathcal{M}_{IMI} + \mathcal{M}_{MIM})]$$
$$- \mathrm{i}R_{IL}\frac{1}{F^{(2)}_{ILMN}}[\mathcal{M}_{ILJ}(\mathcal{M}_{IIL} + \mathcal{M}_{LLI}) + \mathcal{M}_{JJL}(\mathcal{M}_{ILI} + \mathcal{M}_{LIL})]$$
$$- \mathrm{i}R_{IK}\frac{1}{F^{(3)}_{IKLMN}}[\mathcal{M}_{IKJ}(\mathcal{M}_{IIK} + \mathcal{M}_{KKI}) + \mathcal{M}_{JJK}(\mathcal{M}_{IKI} + \mathcal{M}_{KIK})]\Big\}, \tag{18}$$

with $f(x) = \sqrt{x}[1-(1+x)\ln(1+1/x)]$ being the loop function, $\mathcal{M}_{IJK} \equiv M_I A_{JK}$ and

$$A_{IJ} = \frac{(h^\dagger h)^*_{IJ}}{16\pi}, \qquad R_{IJ} = \frac{M_I^2}{M_I^2 - M_J^2 + 2\mathrm{i}M_I^2 A_{JJ}},$$
$$F^{(1)}_{IJK} = 1 + 2\mathrm{i}\,\mathrm{Im}(R_{IK})T_{IJK},$$
$$F^{(2)}_{IJKL} = F^{(1)}_{IJL} + 2\mathrm{i}\,\mathrm{Im}\left(R_{IK}\frac{1}{F^{(1)}_{IKL}}\right)T_{IJK},$$
$$F^{(3)}_{IJKLM} = F^{(2)}_{IJLM} + 2\mathrm{i}\,\mathrm{Im}\left(R_{IK}\frac{1}{F^{(2)}_{IKLM}}\right)T_{IJK},$$
$$F^{(4)}_{IJKLMN} = F^{(3)}_{IJLMN} + 2\mathrm{i}\,\mathrm{Im}\left(R_{IK}\frac{1}{F^{(3)}_{IKLMN}}\right)T_{IJK},$$
$$T_{IJK} = \frac{M_I^2|A_{JK}|^2 + M_J M_K \mathrm{Re}A^2_{JK}}{M_I^2 - M_J^2 + 2\mathrm{i}M_I^2 A_{JJ}}. \tag{19}$$

The corresponding CP-conjugate effective Yukawa couplings $(\bar{h})_{\alpha I}$ can be obtained by simply making the replacements $h_{\alpha I} \to h^*_{\alpha I}$ in the above expressions. Furthermore, in terms of these effective Yukawa couplings, the decay widths of sterile neutrinos can be expressed as

$$\Gamma(N_I \to L_\alpha + H) = \frac{M_I}{16\pi}|(\bar{h}_+)_{\alpha I}|^2,$$
$$\Gamma(N_I \to \bar{L}_\alpha + \bar{H}) = \frac{M_I}{16\pi}|(\bar{h}_-)_{\alpha I}|^2. \tag{20}$$

Therefore, the flavor-specific CP asymmetries for the decays of the Ith sterile neutrino are given by

$$\varepsilon_{I\alpha} = \frac{|(\bar{h}_+)_{\alpha I}|^2 - |(\bar{h}_-)_{\alpha I}|^2}{(\bar{h}^\dagger_+\bar{h}_+)_{II} + (\bar{h}^\dagger_-\bar{h}_-)_{II}}. \tag{21}$$

In the standard seesaw models, the interactions of the unstable heavy neutrinos can be effectively described within the framework of $\Delta L = 2$ scattering processes mediated by on-shell heavy neutrinos $L_\alpha\Phi \leftrightarrow L^C_\beta\Phi^\dagger$. These scatterings can be separated into on-shell and off-shell contributions, where the former yields the inverse decay process. The corresponding reaction density is given by

$$\gamma^{\mathrm{on}}_{\Delta L=2,I\alpha} = \frac{\gamma^D_{I\alpha}}{4} \equiv \frac{1}{4}n^{\mathrm{eq}}_{N_I}\frac{\mathcal{K}_1}{\mathcal{K}_2}\Gamma_{I\alpha}$$
$$= \frac{4}{z}\frac{M_I^4}{246\pi^3}(|(\bar{h}_+)_{\alpha I}|^2 + |(\bar{h}_-)_{\alpha I}|^2)\mathcal{K}_1(zM_I/M_1), \tag{22}$$

where $\mathcal{K}_{1,2}(z)$ are the modified Bessel functions, $z \equiv M_1/T$ with T being the thermal bath temperature, and $\Gamma_{I\alpha} = \Gamma(N_I \to L_\alpha + H) + \Gamma(N_I \to \bar{L}_\alpha + \bar{H})$. The strength of washout effects due to inverse decays is controlled by the washout parameters

$$K_\alpha = \sum_I K_{I\alpha} = \sum_I \frac{\Gamma_{I\alpha}}{H(T = M_I)}, \tag{23}$$

where $H(T) = 1.66\sqrt{g_*}T^2/M_{\mathrm{Pl}}$ is the Hubble rate, g_* the number of relativistic degrees of freedom, and $M_{\mathrm{Pl}} = 1.22 \times 10^{19}$ GeV the Planck mass, but in the ISS model, it is natural to expect that the lepton-number-violating washout will go to zero in the limit of vanishing μ_s; and it has been shown that the suppression of the washout proceeds through the destructive interference of one member of a PD sterile neutrino pair with the other, leaving a washout which vanishes in the lepton-number-conserving (LNC) limit (i.e., $\mu_s = 0$) [53,59]. The total washout is protected by the symmetry and vanishes exactly in the LNC limit, regardless of the large values in the naive parameters of Eq. (23). The introduction of a sizable μ_s breaks this protective symmetry, breaking the cancellation and restoring the standard inverse-decay washout. This highlights the critical role of interference effects, which are absent in standard seesaw models but paramount in approximate LNC frameworks like the ISS model. Following the treatment proposed in Ref. [53], one must return to the fundamental definition of $\Delta L = 2$ scattering reaction density,

$$\gamma^{\mathrm{tot}}_{\Delta L=2,\alpha} = \frac{1}{z}\frac{M_1^4}{64\pi^4}\int_{x_{\mathrm{thr}}}^\infty dx\sqrt{x}\hat{\sigma}_{\Delta L=2,\alpha}(x)\mathcal{K}_1(z\sqrt{x}), \tag{24}$$

where $x \equiv s/M^2_{N_1}$, and x_{thr} denotes the kinematic threshold. The s-channel reduced cross section is given by [57]

$$\hat{\sigma}_{\Delta L=2,\alpha}(x) = \sum_{\beta=1}^3\sum_{I,J=1}^6 \mathrm{Re}\Big\{\Big[(\bar{h}_+)^*_{\alpha I}(\bar{h}_+)_{\alpha J}(\bar{h}_+)^*_{\beta I}(\bar{h}_+)_{\beta J}$$
$$+ (\bar{h}_-)^*_{\alpha I}(\bar{h}_-)_{\alpha J}(\bar{h}_-)^*_{\beta I}(\bar{h}_-)_{\beta J}\Big]\frac{x\sqrt{a_I a_J}}{4\pi P^*_I P_J}\Big\}, \tag{25}$$

where $P_I^{-1} = (x - a_I + i\sqrt{a_I c_I})^{-1}$ is the Breit-Wigner s-channel propagator, with $a_I = (M_I/M_1)^2$ and $c_I = (\Gamma_I/M_1)^2$. A key advantage of this expression is that the cross section naturally incorporates the interference terms among different heavy neutrinos, thereby enabling a consistent definition of the effective washout parameter as

$$K^{\mathrm{eff}}_\alpha \equiv K_\alpha \cdot \frac{\gamma^{\mathrm{tot}}_{\Delta L=2,\alpha}}{\gamma^D_\alpha/4}, \tag{26}$$

where $\gamma^D_\alpha \equiv \sum_I^6 \gamma^D_{I\alpha}/6$.

In most of realistic leptogenesis parameter space, one has $K^{\mathrm{eff}}_\alpha \gtrsim 1$, known as the strong washout regime. In this regime, the efficiency factors are roughly inversely proportional to the washout parameter, as described by

$$\kappa_\alpha \approx \frac{2}{z_B K^{\mathrm{eff}}_\alpha}\left[1 - e^{-\frac{1}{2}z_B K^{\mathrm{eff}}_\alpha}\right], \tag{27}$$

where z_B is well approximated by [60]

$$z_B \approx 1 + \frac{1}{2}\ln\left[1 + \frac{\pi K_\alpha^{\rm eff\,2}}{1024}\left(\ln\frac{3125\pi\, K_\alpha^{\rm eff\,2}}{1024}\right)^5\right]. \quad (28)$$

For completeness, we also consider the weak washout regime where $K_\alpha^{\rm eff} < 1$. In this regime, depending on whether K_α is larger or smaller than 1, there are the following two distinct cases:

$$\kappa_\alpha \approx \begin{cases} \frac{1}{4} K_\alpha^{\rm eff}\left(\frac{3\pi}{2} - z_B\right) & (K_\alpha > 1); \\ \frac{9\pi^2}{64} K_\alpha^{\rm eff} K_\alpha & (K_\alpha < 1). \end{cases} \quad (29)$$

Finally, with the help of Eq. (21), we show that for the ISS model with $M_{\rm R}$ in Eq. (7) and $\mu_{\rm s}$ in Eq. (8) the total CP asymmetries (summed over the sterile neutrinos) are greatly suppressed. Let us take the first PD pair of sterile neutrinos (which contains the first and fourth sterile neutrinos) as an example: the relation $V_1 = {\rm i}V_2$ holds in the present scenario [see Eq. (11)], and it implies

$$h_{\alpha 1} = i h_{\alpha 4}, \qquad \mathcal{V}_{\alpha 1} = i\mathcal{V}_{\alpha 4},$$
$$(\mathcal{B}_+)_{\alpha 1} \simeq i(\mathcal{B}_-)^*_{\alpha 4}, \qquad (\mathcal{B}_-)_{\alpha 1} \simeq i(\mathcal{B}_+)^*_{\alpha 4}, \quad (30)$$

where $(\mathcal{B}_+)_{\alpha I} = \sum_{J,K,L,M,N=1}^{6} h_{\alpha J}\mathcal{F}_{IJKLMN}$ (while $(\mathcal{B}_-)_{\alpha I}$ can be obtained by making the replacement $h_{\alpha I} \to h^*_{\alpha I}$). It follows that

$$|(\bar{h}_+)_{\alpha 1}|^2 \approx |(\bar{h}_-)_{\alpha 4}|^2, \qquad |(\bar{h}_-)_{\alpha 1}|^2 \approx |(\bar{h}_+)_{\alpha 4}|^2, \quad (31)$$

and, consequently, $\varepsilon_{1\alpha}$ and $\varepsilon_{4\alpha}$ cancel each other out to the leading order. Therefore, the total CP asymmetry for the first PD pair of sterile neutrinos is greatly suppressed, and the same is true for the other two pairs of PD sterile neutrinos. This is why we need to break the degeneracies among different PD sterile neutrino pairs in order to potentially achieve sufficient baryon asymmetry.

III. RENORMALIZATION GROUP EVOLUTION ASSISTED LEPTOGENESIS

In this section, we study the scenario that the desired mass splittings among different PD sterile neutrino pairs are generated from the RGE effects. In this scenario, as we will see, it is the differences among the Yukawa couplings of different RHNs that induce mass splittings among different PD sterile neutrino pairs.

A. Consequence for leptogenesis

In the literature, the flavor symmetries are usually placed at very high energy scales $\Lambda_{\rm FS}$ [37–38]. When dealing with leptogenesis, which takes place around the sterile neutrino mass scale M_0, the RGE effects should be taken into account if there is a large gap between $\Lambda_{\rm FS}$ and M_0. In the SM framework, the one-loop RGE equations of the neutrino Yukawa coupling matrix Y_ν and the mass matrix $M_{\rm R}$ are described by [61]

$$16\pi^2 \frac{{\rm d}Y_\nu}{{\rm d}t} = \left(\alpha_\nu - \frac{3}{2}Y_l Y_l^\dagger + \frac{3}{2}Y_\nu Y_\nu^\dagger\right)Y_\nu,$$
$$16\pi^2 \frac{{\rm d}M_{\rm R}}{{\rm d}t} = M_{\rm R}Y_\nu^\dagger Y_\nu + Y_\nu^{\rm T} Y_\nu^* M_{\rm R}, \quad (32)$$

where $t = \ln(\mu/\Lambda_{\rm FS})$ has been defined with μ being the renormalization scale. The parameter α_ν is defined as

$$\alpha_\nu = {\rm tr}\left(3Y_u Y_u^\dagger + 3Y_d Y_d^\dagger + Y_l Y_l^\dagger + Y_\nu Y_\nu^\dagger\right) - \frac{9}{20}g_1^2 - \frac{9}{4}g_2^2, \quad (33)$$

where g_1 and g_2 are the ${\rm U}(1)_{\rm Y}$ and ${\rm SU}(2)_{\rm L}$ gauge coupling constants, and $Y_{u,d,l}$ are, respectively, the Yukawa matrices for up-type quarks, down-type quarks, and charged leptons.

Before performing the numerical calculations, for the purpose of illustration, we take the diagonal terms of $M_{\rm R}$ as an example to show the impacts of RGE effects on leptogenesis. For the II element of $M_{\rm R}$, an integration of Eq. (32) yields the following relation between its value at the flavor-symmetry scale $\Lambda_{\rm FS}$ and mass scale M_0:

$$M_{II}(M_0) \simeq M_{II}(\Lambda_{\rm FS})\left[1 - \frac{1}{16\pi^2}\left(Y_\nu^\dagger Y_\nu\right)_{II}\ln\left(\frac{\Lambda_{\rm FS}}{M_0}\right)\right], \quad (34)$$

which yields the following splitting between $M_{II}(M_0)$ and $M_{JJ}(M_0)$:

$$M_{II}(M_0) - M_{JJ}(M_0) \simeq \frac{M_I(\Lambda_{\rm FS})}{16\pi^2}\left[\left(Y_\nu^\dagger Y_\nu\right)_{JJ} - \left(Y_\nu^\dagger Y_\nu\right)_{II}\right]\ln\left(\frac{\Lambda_{\rm FS}}{M_0}\right). \quad (35)$$

This shows that it is really the differences among the Yukawa couplings of different RHNs that induce mass splittings among different PD sterile neutrino pairs, as mentioned above. One can also see that such mass splittings increase significantly as the mass scale μ_0 decreases [accompanying which the magnitudes of Y_ν will increase as indicated by Eq. (5)], potentially exceeding the scale of μ_0 itself. At this point, although the Yukawa coupling matrix still satisfies the relationship described in Eq. (30), the $(\mathcal{B}_\pm)_{\alpha I}$ terms no longer do so. Consequently, the cancellation of CP asymmetries is weakened, allowing for the potential generation of a sufficiently large baryon asymmetry. Finally, we stress that the off-diagonal-term contributions are also significant in the scenario considered in this paper, and we have also taken account of them in the following calculations.

Now, we are ready to perform the numerical calculations. In Figs. 1(a) and 1(b) (for the normal ordering (NO) and inverted ordering (IO) cases of light neutrino masses,

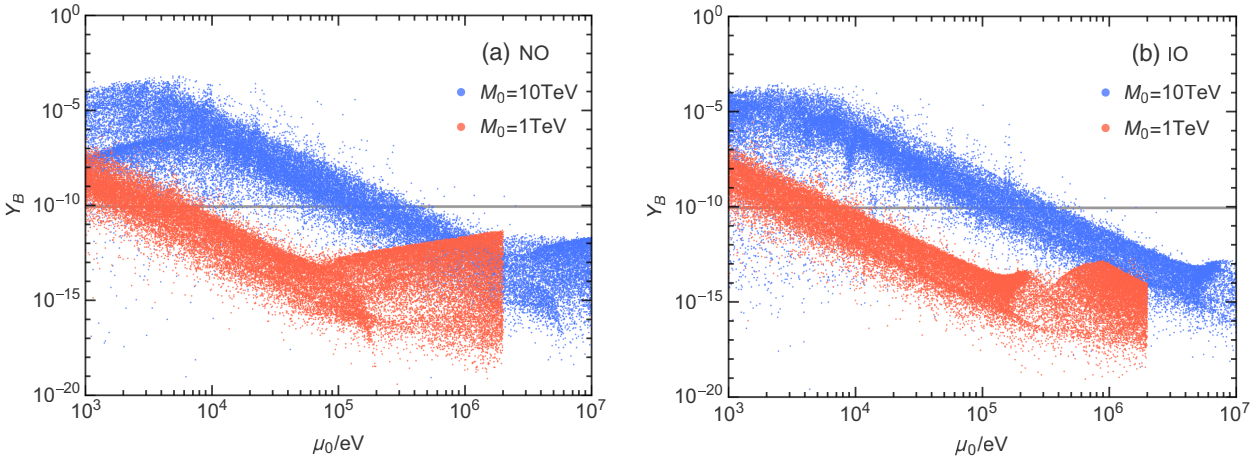


FIG. 1. For the scenario studied in Sec. III A, in the NO (a) and IO (b) cases, the allowed values of $Y_{\rm B}$ as functions of μ_0 for some benchmark values of M_0. The horizontal line stands for the observed value of $Y_{\rm B}$.

respectively) we have shown the allowed values of $Y_{\rm B}$ as functions of μ_0 for the benchmark values of $M_0 = 1$ and 10 TeV. These results are obtained for the following parameter settings: for the neutrino mass squared differences and neutrino mixing angles, we employ the global-fit results for them [32,33]. For the two Majorana CP phases of the neutrino mixing matrix, we allow them to vary in the range $0 - 2\pi$, while the Dirac CP phase is constrained by the TM1 mixing scheme realized by the scenario considered in the present paper. The lightest neutrino mass (m_1 or m_3 in the NO or IO case) is varied in the range between 0.001 eV and 0.1 eV. For $\Lambda_{\rm FS}$, we fix $\Lambda_{\rm FS}/M_0 = 10^2$ as a benchmark value (in fact, the dependence of the final results on it is weak since the RGE effects only depend on it in a logarithmic manner). To conform to the essential idea of the ISS model (i.e., $\mu_{\rm s} \ll M_{\rm D} \ll M_{\rm R}$), in the calculations we have required $\mu_{\rm s}$ to be at least 2 orders of magnitude smaller than $M_{\rm D}$, and $M_{\rm D}$ to be at least 2 orders of magnitude smaller than $M_{\rm R}$.

The results show that in both the NO and IO cases the observed value of $Y_{\rm B}$ has a chance to be successfully reproduced. It is clear that for smaller values of M_0 (e.g., $M_0 = 1$ TeV), relatively small values of μ_0 (around 10^3 eV) are needed to reproduce the observed value of $Y_{\rm B}$. As M_0 increases, the scale of μ_0 needed to reproduce the observed $Y_{\rm B}$ also rises. In the figure, two turning points are observed. Upon further analysis, we find that for $M_0 = 10$ TeV, the left turning point results from a decrease in μ_0, leading to an increase in the sterile neutrino mass splittings induced by the RGE effects. Once these splittings become too large, significant hierarchies among the three PD sterile neutrino pairs arise. In particular, around $\mu_0 \sim 10^3$ eV, only one PD pair remains quasidegenerate (under the degeneracy criterion of $\Delta M/M \lesssim 10^{-3}$ adopted in this work), effectively reducing the system to a two-state resonance. As a result, the six-state framework underlying Eq. (18) is no longer realized. We emphasize that this conclusion is determined by the specific numerical threshold used to define quasidegeneracy. Our stringent choice ensures that Eq. (18) only applies within a fully controlled six-state scenario, thereby placing the region near the left turning point outside the valid domain of our analysis. Conversely, the right turning point occurs due to an increase in μ_0, which causes the sterile neutrino mass splittings induced by the RGE effects to approach the scale of μ_0. In this regime, μ_0 also contributes significantly and is equally important. In the six-state scenario with three PD pairs, the pattern of the resonant enhancement is more intricate than in the conventional two-state case. The right turning point appears when the mass splittings of each PD pair (controlled by μ_0) become comparable to their decay widths, so that each PD pair can individually enter their own resonant regime. By contrast, the earlier enhancement region is dominated by the mass splittings among different PD pairs. It is worth noting that even in the standard two-state case, resonant leptogenesis does not merely feature a single resonance regime but can exhibit multiple enhancement regimes depending on the relative sizes of the mass splittings and decay widths. Overall, it can be observed that as M_0 varies in the range of 1 to 10 TeV, the observed value of $Y_{\rm B}$ can be successfully reproduced across a wide scale of μ_0, spanning from 10^3 to 10^6 eV.

B. Charged lepton flavor violation

In the context of our model, the Yukawa interactions responsible for generating neutrino masses also give rise to charged lepton flavor violation (cLFV). Among various possible cLFV channels, the radiative decay $l_\alpha \to l_\beta \gamma$ is the most widely studied one, as it provides the most stringent experimental limits and is expected to exhibit the largest branching ratios. According to the MEG Collaboration [62], one now has the experimental limit $\mathrm{BR}(\mu \to e\gamma) < 4.2 \times 10^{-13}$. Therefore, the evaluation of branching ratios for these decays within our framework not only acts as a key

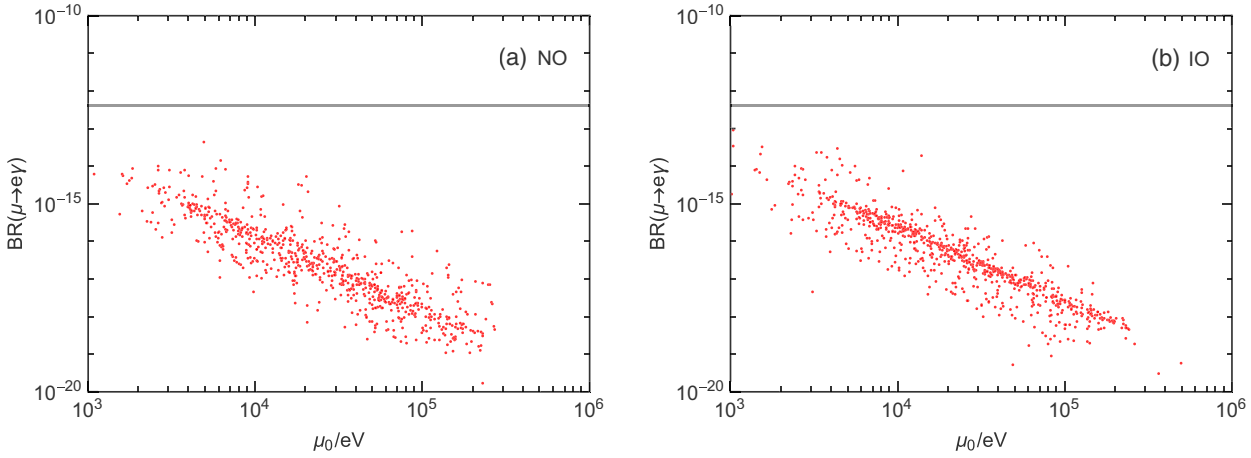


FIG. 2. For the scenario studied in Sec. III A, in the parameter space that allows for a reproduction of the observed value of Y_{B}, the allowed values of $\mathrm{BR}(\mu \to e\gamma)$ as functions of μ_0 in the NO (a) and IO (b) cases. The horizontal line stands for the current upper bound on $\mathrm{BR}(\mu \to e\gamma)$.

consistency check of the model but also establishes a direct connection between the neutrino mass generation mechanism and experimentally accessible low-energy signals.

Within our framework, $\mathrm{BR}(l_\alpha \to l_\beta\gamma)$ can be calculated according to [63]

$$\mathrm{BR}(l_\alpha \to l_\beta\gamma) = \frac{\alpha_W^3 s_W^2}{256\pi^2}\frac{m_{l_\alpha}^5}{M_W^4}\frac{1}{\Gamma_{l_\alpha}}|G_{\alpha\beta}^W|^2, \tag{36}$$

where

$$G_{\alpha\beta}^W = \sum_{i=1}^{9} K_{\alpha i}^* K_{\beta i} G_\gamma^W\left(\frac{M_i^2}{M_W^2}\right),$$
$$G_\gamma^W(x) = \frac{1}{12(1-x)^4}(10 - 43x + 78x^2 - 49x^3 + 18x^3\ln x + 4x^4). \tag{37}$$

Here $\alpha_W \equiv g_W^2/(4\pi)$ denotes the weak fine-structure constant, $s_W^2 = \sin^2\theta_W$, with θ_W being the Weinberg angle, M_W the W-boson mass, m_{l_α} and Γ_{l_α} the mass and total decay width of the decaying charged lepton l_α. Finally, one has the matrix $K = (K_L, K_H)$ with

$$K_L = \left(I - \frac{1}{2}(M_{\mathrm{D}}, 0)^*(M_{NS}'^{-1})^* M_{NS}'^{-1}(M_{\mathrm{D}}, 0)^T\right)U'^*,$$
$$K_H = (M_{\mathrm{D}}, 0)^*(M_{NS}'^{-1})^* V, \tag{38}$$

where M'_{NS} is the sterile-neutrino mass matrix after taking account of the RGE effects.

Now we investigate the consequences of the model with respect to the $\mu \to e\gamma$ process. In Figs. 2(a) and 2(b) (for the NO and IO cases, respectively), we have shown the allowed values of $\mathrm{BR}(\mu \to e\gamma)$ as functions of μ_0. With the same parameter settings as in Sec. III A, these results are obtained within the parameter space that allows for a successful reproduction of the observed baryon asymmetry of the Universe, with M_1 varying in the range from 1 to 10 TeV. It turns out that, for the parameter space consistent with the observed value of Y_{B}, the allowed values of $\mathrm{BR}(\mu \to e\gamma)$ are well below the current upper bound.

IV. NONTRIVIAL FLAVOR STRUCTURE OF μ_{s} ASSISTED LEPTOGENESIS

In this section, we study the scenario that the μ_{s} matrix also contains some nontrivial flavor structure parallel to that in Eq. (9). With the help of Eq. (4), utilizing the light neutrino mass matrix and the M_{D} matrix, we can derive the μ_{s} matrix accordingly. This derivation allows us to proceed with the subsequent calculations of baryon asymmetry.

We will consider two distinct scenarios. In the first scenario, we simply assume that there exists no gap between the energy scale underlying the ISS model and the sterile neutrino mass scale so that the RGE effects can be safely neglected, in which case we just need to consider the contributions of the nontrivial flavor structure of μ_{s} to the mass splittings among different PD sterile neutrino pairs. By introducing nontrivial flavor structure for μ_{s}, distinctions among the three S_I singlets arise, effectively breaking the mass degeneracies among the three PD sterile neutrino pairs. Consequently, the $(\mathcal{B}_\pm)_{\alpha I}$ terms no longer satisfy the relationship in Eq. (30). Additionally, as in previous calculations, we need to diagonalize the sterile neutrino mass matrix to conveniently calculate the generated baryon asymmetry. However, in the present scenario, the nontrivial flavor structure of μ_{s} adds complexity to the diagonalization process and alters the structure of the unitary matrices involved. Specifically, the unitary matrices V_1 and V_2 in Eq. (11) will exhibit notable differences and cannot be simply related by the relation $V_1 = \mathrm{i}V_2$ [which holds in the case that μ_s takes a simple form as shown

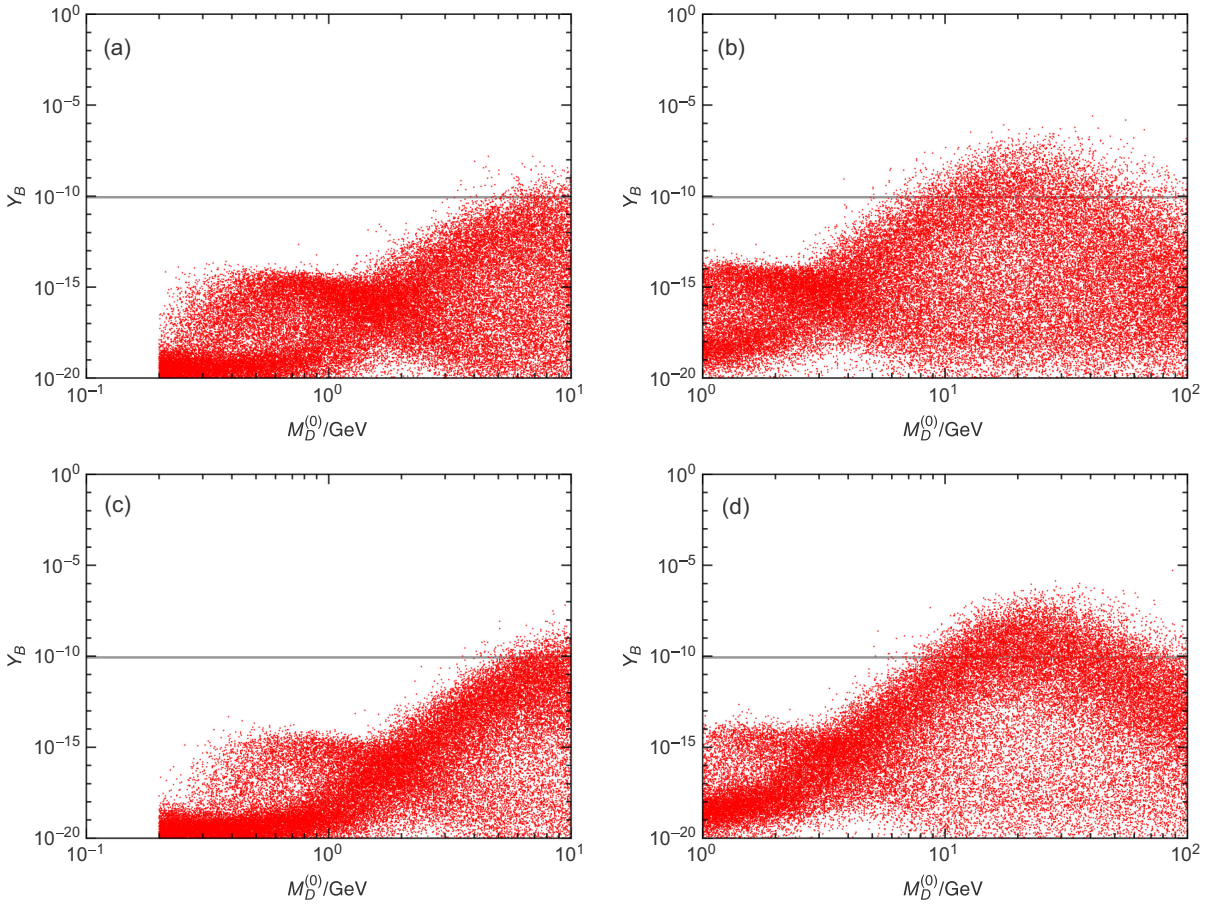


FIG. 3. For the first scenario studied in Sec. IV where we only consider the contributions of the nontrivial flavor structure of μ_s to the mass splittings among different PD sterile neutrino pairs, in the NO (IO) case, the allowed values of Y_B as functions of $M_D^{(0)}$ for some benchmark values of M_0. The horizontal line stands for the observed value of Y_B. (a) NO $M_0 = 1$ TeV, (b) NO $M_0 = 10$ TeV, (c) IO $M_0 = 1$ TeV, (d) IO $M_0 = 10$ TeV.

in Eq. (8)]. Subsequently, the Yukawa coupling matrices are no longer constrained by the relationships outlined in Eq. (30). As a result, the cancellations for the total CP asymmetry will be weakened, enhancing the potential to generate a sufficiently large baryon asymmetry.

For the present scenario, Fig. 3 has shown the allowed values of Y_B as functions of $M_D^{(0)}$ (the common overall scale of M_D) for the benchmark values of $M_0 = 1$ and 10 TeV. These results are obtained for the following parameter settings: for the neutrino mass squared differences and neutrino mixing angles, we employ the global-fit results for them [32,33]. For the two Majorana CP phases of the neutrino mixing matrix, we allow them to vary in the range $0 - 2\pi$, while the Dirac CP phase is constrained by the TM1 mixing scheme realized in the scenario considered in this paper. The lightest neutrino mass (m_1 or m_3 in the NO or IO case) is varied in the range between 0.001 eV and 0.1 eV. To maintain the general form of M_D, we allow the absolute values of its matrix elements to fluctuate within a range of 0.5 to 2 times $M_D^{(0)}$. To conform to the essential idea of the ISS model, we require μ_s to be at least 2 orders of magnitude smaller than M_D, and M_D to be at least 2 orders of magnitude smaller than M_R. The results show that in both the NO and IO cases the observed value of Y_B has a chance to be successfully reproduced. It can be seen that the observed value of Y_B has a relatively higher probability of being successfully reproduced for $M_D^{(0)}$ around 1 GeV. Overall, it can be observed that as M_0 varies in the range of 1 to 10 TeV, the observed value of Y_B can be successfully reproduced for $M_D^{(0)}$ in the range of 1 to 10 GeV. For this scenario, we have also investigated the consequences of the model with respect to the $\mu \to e\gamma$ process. The results are shown in Figs. 4(a) and 4(b) (for the NO and IO cases, respectively). The results show that the parameter range of $M_D^{(0)} \gtrsim 4$ GeV is excluded by the constraint from the $\mu \to e\gamma$ process, leaving us with $2 \lesssim M_D^{(0)}/\text{GeV} \lesssim 4$. This stronger constraint from $\mu \to e\gamma$, compared to the case with a trivial μ_s structure, stems from the nontrivial flavor structure of μ_s, which modifies the relationship between the diagonalization matrices V_1 and V_2. As a result, the condition $K_{\alpha 1} = iK_{\alpha 4}$ no longer holds within

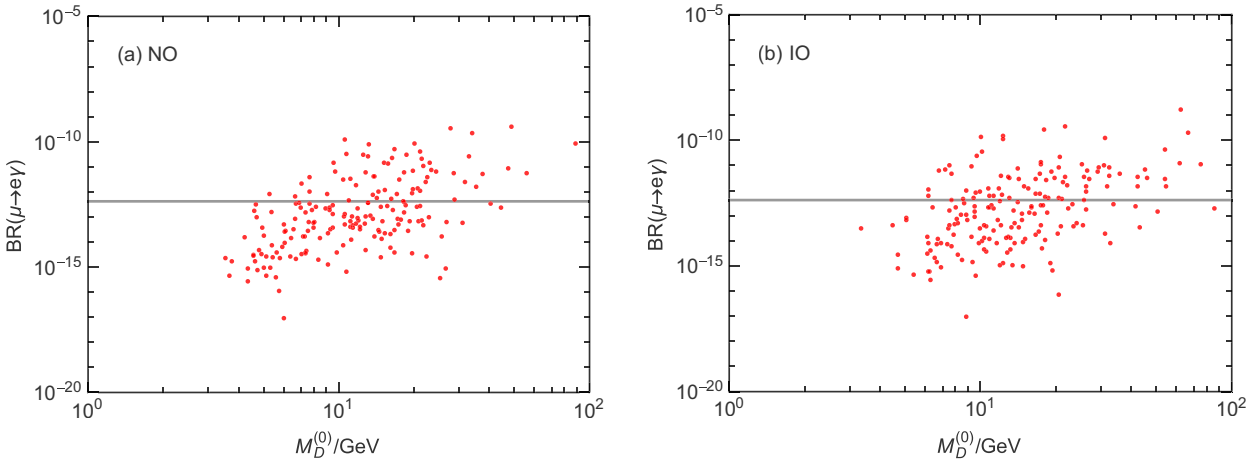


FIG. 4. For the first scenario studied in Sec. IV, in the parameter space that allows for a reproduction of the observed value of $Y_{\rm B}$, the allowed values of $\mathrm{BR}(\mu \to e\gamma)$ as functions of $M_{\rm D}^{(0)}$ in the NO (a) and IO (b) cases. The horizontal line stands for the current upper bound on $\mathrm{BR}(\mu \to e\gamma)$.

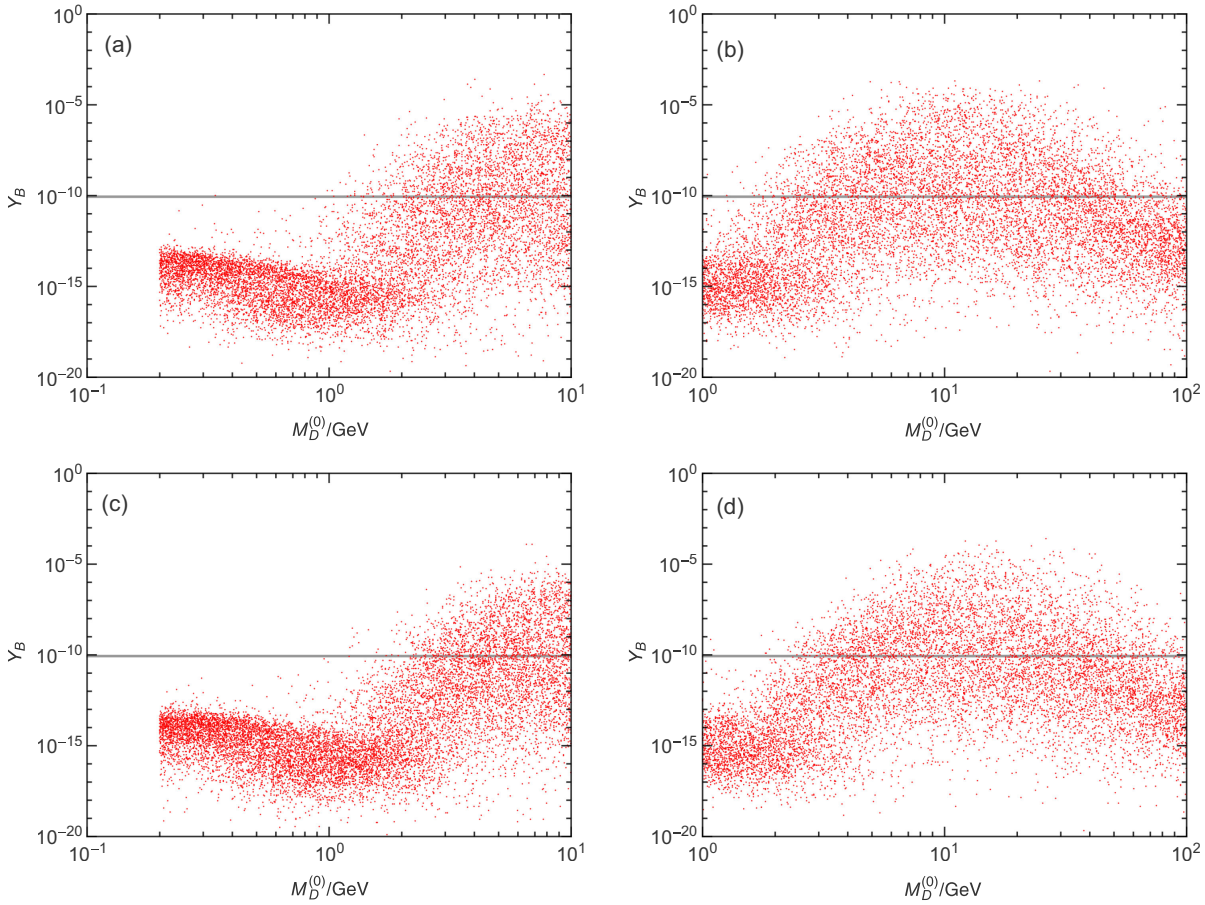


FIG. 5. For the second scenario studied in Sec. IV where we take into account both the contributions of the RGE effects and $\mu_{\rm s}$ to the mass splittings among different PD sterile neutrino pairs, in the NO (IO) case, the allowed values of $Y_{\rm B}$ as functions of $M_{\rm D}^{(0)}$ for some benchmark values of M_0. The horizontal line stands for the observed value of $Y_{\rm B}$. (a) NO $M_0 = 1$ TeV, (b) NO $M_0 = 10$ TeV, (c) IO $M_0 = 1$ TeV, (d) IO $M_0 = 10$ TeV.

each PD pair, thereby weakening the cancellation between their contributions to the cLFV amplitude. This leads to an enhanced branching ratio and, consequently, to a more stringent experimental constraint, bringing this scenario around to the current experimental sensitivity and making it testable.

In the second scenario, we assume that there is a considerable gap between the energy scale underlying the ISS model and the sterile neutrino mass scale so that the RGE effects may become non-negligible. In this case, we take into account both the contributions of the RGE effects and $\mu_{\rm s}$ to the mass splittings among different PD sterile neutrino pairs. Although the contributions of the RGE effects are comparable to or exceed those of $\mu_{\rm s}$, the latter provides an essential contribution. As noted previously, this structure complicates the diagonalization procedure. It is worth reiterating that this leads to notable differences between the unitary matrices V_1 and V_2 in Eq. (11), specifically invalidating the relation $V_1 = {\rm i}V_2$ that holds for the simple form of μ_s in Eq. (8). Consequently, the Yukawa coupling matrices are no longer constrained by the relationships in Eq. (30). For this scenario, we have shown the allowed values of $Y_{\rm B}$ as functions of $M_{\rm D}^{(0)}$ in Figs. 5(a) and 5(b) (for the NO and IO cases, respectively). It is found that the parameter space that allows for a reproduction of the observed value of $Y_{\rm B}$ is broader than that shown in Fig. 3, where only the contributions of $\mu_{\rm s}$ were considered. Overall, it can be observed that as M_0 varies in the range of 1 to 10 TeV, the observed value of $Y_{\rm B}$ can be successfully reproduced for $M_{\rm D}^{(0)}$ in the range of 1 to 10 GeV. Figures 6(a) and 6(b) (for the NO and IO cases, respectively) have shown the consequences of the model with respect to the $\mu \to e\gamma$ process. The results show that the parameter range of $M_{\rm D}^{(0)} \gtrsim 2$ GeV is excluded by the constraint from the $\mu \to e\gamma$ process, leaving us with $1 \lesssim M_{\rm D}^{(0)}/{\rm GeV} \lesssim 2$.

V. SUMMARY

The type-I seesaw mechanism provides an elegant explanation for both the neutrino masses and the baryon asymmetry of the Universe. However, the traditional type-I seesaw mechanism and associated leptogenesis mechanism have the drawback that the newly introduced particle states are too heavy to be directly accessed by foreseeable experiments. In this connection, the ISS model provides an attractive framework that can naturally explain the smallness of neutrino masses while accommodating some sterile neutrinos potentially accessible at present or future experiments. However, in generic ISS models with hierarchical PD sterile neutrino pairs (in which case the resonance effects for leptogenesis only take place within each pair of PD sterile neutrinos, in contrast with the scenario considered in this paper), the generation of the observed baryon asymmetry of the Universe via the leptogenesis mechanism is extremely challenging.

In this paper, we have investigated rescuing leptogenesis in the ISS model with the help of non-Abelian flavor symmetries, which have the potential to explain the observed peculiar neutrino mixing pattern. The basic idea is that the non-Abelian flavor symmetries can naturally enforce mass degeneracies among the three PD sterile neutrino pairs. After these degeneracies are broken in a proper way, resonant leptogenesis among different PD sterile neutrino pairs can naturally arise, potentially enhancing the generated baryon asymmetry. To be concrete, thanks to the non-Abelian flavor symmetries, $M_{\rm R}$ and μ_s can naturally take the forms in Eqs. (7) and (8), which enforce mass degeneracies among the three PD sterile neutrino pairs, while $M_{\rm D}$ can naturally take a form in Eq. (9), which realizes the popular TM1 neutrino mixing. Then, we have considered two well-motivated approaches to generate the desired mass splittings: (i) they can be

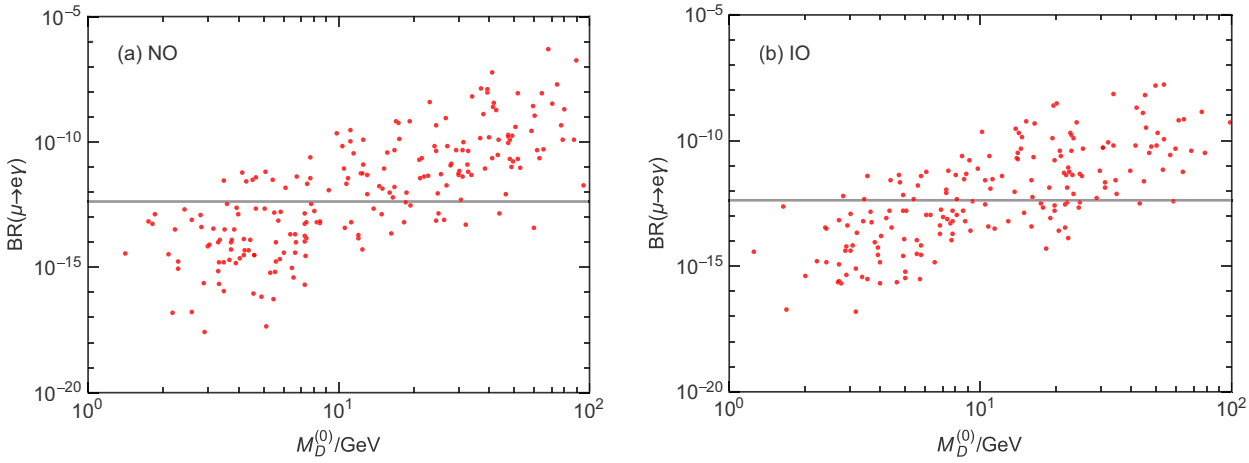


FIG. 6. For the second scenario studied in Sec. IV, in the parameter space that allows for a reproduction of the observed value of $Y_{\rm B}$, the allowed values of ${\rm BR}(\mu \to e\gamma)$ as functions of $M_{\rm D}^{(0)}$ in the NO (a) and IO (b) cases. The horizontal line stands for the current upper bound on ${\rm BR}(\mu \to e\gamma)$.

naturally induced by the RGE effects; (ii) when the mass matrix μ_s also contains some nontrivial flavor structure, the flavor nonuniversality of μ_s will break the mass degeneracies among the three PD sterile neutrino pairs.

In the first scenario, the RGE effects break the mass degeneracies of three RHNs, which finally result in mass splittings among the three PD sterile neutrino pairs. Figures 1(a) and 1(b) demonstrate that in both the NO and IO cases, the observed value of Y_B can be successfully reproduced. For smaller values of M_0 (e.g., $M_0 = 1$ TeV), relatively small values of μ_0 (around 10^3 eV) are needed to reproduce the observed value of Y_B. As M_0 increases, the scale of μ_0 needed to reproduce the observed Y_B also rises. For this scenario, we have also investigated the consequences of the model with respect to the $\mu \to e\gamma$ process. It turns out that, for the parameter space consistent with the observed value of Y_B, the allowed values of $\mathrm{BR}(\mu \to e\gamma)$ are well below the current upper bound.

In the second scenario, the nontrivial flavor structure of μ_s breaks the mass degeneracies of three S_I singlets, which finally result in mass splittings among the three PD sterile neutrino pairs. When we simply assume there exists no gap between the energy scale underlying the ISS model and the sterile neutrino mass scale, the RGE effects can be safely neglected. For this scenario, we have only considered the contributions μ_s to the mass splittings among different PD sterile neutrino pairs. Figure 3 shows that the observed value of Y_B can be successfully reproduced in both the NO and IO cases for $M_D^{(0)}$ in the range of 1 to 10 GeV. When there is a considerable gap between the energy scale underlying the ISS model and the sterile neutrino mass scale, the RGE effects may become non-negligible. For this scenario, we have considered both the contributions of the RGE effects and μ_s. Figure 5 shows that the parameter space that allows for a reproduction of the observed value of Y_B is broader than that shown in Fig. 3, where only the contributions of μ_s were considered. For these two scenarios, it turns out that the constraint from the $\mu \to e\gamma$ process can help us exclude some parameter space that allows for a reproduction of the observed value of Y_B.

ACKNOWLEDGMENTS

This work was supported in part by the National Natural Science Foundation of China under Grant No. 12475112, Liaoning Revitalization Talents Program under Grant No. XLYC2403152, and the Basic Research Business Fees for Universities in Liaoning Province under Grant No. LJ212410165050.

DATA AVAILABILITY

The data that support the findings of this article are not publicly available. The data are available from the authors upon reasonable request.

[1] Z. Z. Xing, Phys. Rep. **854**, 1 (2020).
[2] P. A. R. Ade *et al.* (Planck Collaboration), Astron. Astrophys. **16**, 571 (2014).
[3] P. Minkowski, Phys. Lett. **67B**, 421 (1977).
[4] M. Gell-Mann, P. Ramond, and R. Slansky, in *Supergravity*, edited by P. van Nieuwenhuizen and D. Freedman (North-Holland, Amsterdam, 1979), p. 315.
[5] T. Yanagida, in *Proceedings of the Workshop on the Unified Theory and the Baryon Number in the Universe*, edited by O. Sawada and A. Sugamoto, KEK Report No. 79-18 (Tsukuba, 1979), p. 95.
[6] R. N. Mohapatra and G. Senjanovic, Phys. Rev. Lett. **44**, 912 (1980).
[7] J. Schechter and J. W. F. Valle, Phys. Rev. D **22**, 2227 (1980).
[8] M. Fukugita and T. Yanagida, Phys. Lett. B **174**, 45 (1986).
[9] W. Buchmuller, R. D. Peccei, and T. Yanagida, Annu. Rev. Nucl. Part. Sci. **55**, 311 (2005).
[10] W. Buchmuller, P. Di Bari, and M. Plumacher, Ann. Phys. (Amsterdam) **315**, 305 (2005).
[11] S. Davidson, E. Nardi, and Y. Nir, Phys. Rep. **466**, 105 (2008).
[12] D. Bodeker and W. Buchmuller, Rev. Mod. Phys. **93**, 035004 (2021).
[13] S. Davidson and A. Ibarra, Phys. Lett. B **535**, 25 (2002).
[14] D. Wyler and L. Wolfenstein, Nucl. Phys. **B218**, 205 (1983).
[15] R. N. Mohapatra, Phys. Rev. Lett. **56**, 561 (1986).
[16] G. 't Hooft, NATO Sci. Ser. B **59**, 135 (1980).
[17] A. M. Abdullahi *et al.*, J. Phys. G **50**, 020501 (2023).
[18] A. Das and N. Okada, Phys. Rev. D **88**, 113001 (2013).
[19] L. Wolfenstein, Nucl. Phys. **B186**, 147 (1981).
[20] S. T. Petcov, Phys. Lett. **110B**, 245 (1982).
[21] J. W. F. Valle and M. Singer, Phys. Rev. D **28**, 540 (1983).
[22] M. Kobayashi and C. S. Lim, Phys. Rev. D **64**, 013003 (2001).
[23] A. Pilaftsis, Phys. Rev. D **56**, 5431 (1997).
[24] A. Pilaftsis and T. E. J. Underwood, Nucl. Phys. **B692**, 303 (2004).
[25] M. J. Dolan, T. P. Dutka, and R. R. Volkas, J. Cosmol. Astropart. Phys. 06 (2018) 012.
[26] A. Abada, G. Arcadi, V. Domcke, and M. Lucente, J. Cosmol. Astropart. Phys. 11 (2015) 041.
[27] A. Abada, G. Arcadi, V. Domcke, and M. Lucente, J. Cosmol. Astropart. Phys. 12 (2017) 024.

[28] E. K. Akhmedov, V. A. Rubakov, and A. Y. Smirnov, Phys. Rev. Lett. **81**, 1359 (1998).
[29] T. Asaka and M. Shaposhnikov, Phys. Lett. B **620**, 17 (2005).
[30] A. Mukherjee and A. K. Saha, Phys. Lett. B **849**, 138474 (2024).
[31] K. Agashe, P. Du, M. Ekhterachian, C. S. Fong, S. Hong, and L. Vecchi, J. High Energy Phys. 04 (2019) 029.
[32] I. Esteban, M. C. Gonzalez-Garcia, M. Maltoni, I. Martinez-Soler, J. P. Pinheiro, and T. Schwetz, J. High Energy Phys. 12 (2024) 216.
[33] F. Capozzi, W. Giarè, E. Lisi, A. Marrone, A. Melchiorri, and A. Palazzo, Phys. Rev. D **111**, 093006 (2025).
[34] P. F. Harrison, D. H. Perkins, and W. G. Scott, Phys. Lett. B **530**, 167 (2002).
[35] Z. Z. Xing, Phys. Lett. B **533**, 85 (2002).
[36] G. Altarelli and F. Feruglio, Rev. Mod. Phys. **82**, 2701 (2010).
[37] S. F. King and C. Luhn, Rep. Prog. Phys. **76**, 056201 (2013).
[38] F. Feruglio and A. Romanino, Rev. Mod. Phys. **93**, 015007 (2021).
[39] G. J. Ding and S. F. King, Rep. Prog. Phys. **87**, 084201 (2024).
[40] G. J. Ding and J. W. F. Valle, Phys. Rep. **1109**, 1 (2025).
[41] J. D. Bjorken, P. F. Harrison, and W. G. Scott, Phys. Rev. D **74**, 073012 (2006).
[42] Z. Z. Xing and S. Zhou, Phys. Lett. B **653**, 278 (2007).
[43] X. G. He and A. Zee, Phys. Lett. B **645**, 427 (2007).
[44] C. H. Albright and W. Rodejohann, Eur. Phys. J. C **62**, 599 (2009).
[45] C. H. Albright, A. Dueck, and W. Rodejohann, Eur. Phys. J. C **70**, 1099 (2010).
[46] C. C. Li and G. J. Ding, Nucl. Phys. **B881**, 206 (2014).
[47] F. Feruglio, C. Hagedorn, and R. Ziegler, Eur. Phys. J. C **74**, 2753 (2014).
[48] G. J. Ding, S. F. King, C. Luhn, and A. J. Stuart, J. High Energy Phys. 05 (2013) 084.
[49] T. Nomura, H. Okada, and S. Patra, Nucl. Phys. **B967**, 115395 (2021).
[50] T. P. Nguyen, T. T. Thuc, D. T. Si, T. T. Hong, and L. T. Hue, Prog. Theor. Exp. Phys. **2022**, 023B01 (2022).
[51] C. Hagedorn, J. Kriewald, J. Orloff, and A. M. Teixeira, Eur. Phys. J. C **82**, 194 (2022).
[52] B. Karmakar and A. Sil, Phys. Rev. D **96**, 015007 (2017).
[53] S. Blanchet, T. Hambye, and F. X. Josse-Michaux, J. High Energy Phys. 04 (2010) 023.
[54] A. Abada, S. Davidson, F. X. Josse-Michaux, M. Losada, and A. Riotto, J. Cosmol. Astropart. Phys. 04 (2006) 004.
[55] E. Nardi, Y. Nir, E. Roulet, and J. Racker, J. High Energy Phys. 01 (2006) 164.
[56] A. Pilaftsis and T. E. J. Underwood, Nucl. Phys. **B692**, 303 (2004).
[57] A. Pilaftsis and T. E. J. Underwood, Phys. Rev. D **72**, 113001 (2005).
[58] P. C. da Silva, D. Karamitros, T. McKelvey, and A. Pilaftsis, J. High Energy Phys. 11 (2022) 065.
[59] S. Blanchet, P. S. Bhupal Dev, and R. N. Mohapatra, Phys. Rev. D **82**, 115025 (2010).
[60] W. Buchmuller, P. Di Bari, and M. Plumacher, Ann. Phys. (Amsterdam) **315**, 305 (2005).
[61] J. Bergstrom, M. Malinsky, T. Ohlsson, and H. Zhang, Phys. Rev. D **81**, 116006 (2010).
[62] A. M. Baldini *et al.* (MEG Collaboration), Eur. Phys. J. C **76**, 434 (2016).
[63] D. V. Forero, S. Morisi, M. Tortola, and J. W. F. Valle, J. High Energy Phys. 09 (2011) 142.